JOURNAL OF Applied Polymer SCIENCE

Special Issue: Green and Sustainable Polyurethanes for Advanced Applications

Guest Editors: Prof. Sophie Guillaume (Universite de Rennes, France), Dr. Hamdy Khalil (Woodbridge Foam Corp., Canada), Prof. Manjusri Misra (University of Guelph, Canada)



EDITORIAL

Green and sustainable polyurethanes for advanced applications

Sophie Guillaume, Hamdy Khalil, Manjusri Misra, *J. Appl. Polym. Sci.* 2017, DOI: 10.1002/app.45646

RESEARCH ARTICLES

Polyurethanes prepared from cyclocarbonated broccoli seed oil (PUcc): New biobased organic matrices for incorporation of phosphorescent metal nanocluster
Patrick Loulergue, Maria Amela-Cortes, Stephane Cordier, Yann Molard, Loic Lemiegre, Jean-Luc Audic, *J. Appl. Polym. Sci.* 2017, DOI: 10.1002/app.45339

Non-isocyanate polyurethanes from six-membered cyclic carbonates: Catalysis and side reactions
Robert H. Lambeth, Sanyo M. Matthew, MyVan H. Baranoski, Kathleen J. Housman, Bao Tran, Jonathan M. Oyler, *J. Appl. Polym. Sci.* 2017, DOI: 10.1002/app.44941

Hydrogen bonds prevent obtaining high molar mass PHUs
Blain Marine, Adrien Cornille, Bernard Boutevin, Remi Auvergne, Dominique Benazet, Bruno Andrioletti, Sylvain Caillol, *J. Appl. Polym. Sci.* 2017, DOI: 10.1002/app.44958

Tuning the properties of segmented polyhydroxyurethanes via chain extender structure
Goliath Beniah, William H. Heath, Junho Jeon, John M. Torkelson, *J. Appl. Polym. Sci.* 2017, DOI: 10.1002/app.44942

Structural effects on the reprocessability and stress relaxation of cross-linked polyhydroxyurethanes
David J. Fortman, Jacob P. Brutman, Marc A Hillmyer, William R. Dichtel, *J. Appl. Polym. Sci.* 2017, DOI: 10.1002/app.44984

Non-isocyanate thermoplastic polyurethanes elastomers (NIPUs) based on PEG through the transurethanization approach
Nasreddine Kebir, Soumaya Nouigues, Pierre Moranne, Fabrice Burel, *J. Appl. Polym. Sci.* 2017, DOI: 10.1002/app.44991

Bio-based flexible polyurethane foams derived from succinic polyol: Mechanical and acoustic performances
Maria Oliviero, letizio Verdolotti, Mariamelia Stanzione, Marino Lavorgna, Salvatore Iannace, Maurizio Tarello, Andrea Sorrentino, *J. Appl. Polym. Sci.* 2017, DOI: 10.1002/app.45113

Impact of hard segment concentration on highly resilient polyurethane foams based on palm olein polyol
Srihanum Adnan, Maznee T. I. Tuan Noor, Nurul H. Ain, Kosheela P. P. Devi, Norhisham S. Mohd, Yeong Shoot Kian, Zainab B. Idris, Irma Campara., Christi M. Schiffman, Karol Pietrzyk, Vahid Sendijarevic, Ibrahim Sendijarevic, *J. Appl. Polym. Sci.* 2017, DOI: 10.1002/app.45440

Antimicrobial polyurethane foams having cationic ammonium groups
Esther Udabe, Mehmet Isik, Haritz Sardon, David Mecerreyes, Lourdes Irusta, Maitane Salsamendi, Feng Yan, *J. Appl. Polym. Sci.* 2017, DOI: 10.1002/app.45473

Polyurethane/esterified cellulose nanocrystal composites as a transparent moisture barrier coating for encapsulation of dye sensitized solar cells
Kitti Yuwawech, Jatuphorn Wootthikanokkhan, Sompit Wanwong, Supachok Tanpichai, *J. Appl. Polym. Sci.* 2017, DOI: 10.1002/app.45010

Hydrophobic-hydrophilic surface switching properties of non-chain extended poly(urethane)s for use in agriculture to minimize soil water evaporation and permit water infiltration
Priscilla Johnston, George Freischmidt, Christopher D. Easton, Mark Greaves, Phillip S. Casey, Keith L. Bristow, Pathiraja A Gunatillake, Raju Adhikari, *J Appl. Polym. Sci.* 2017, DOI: 10.1002/app.44756

Preparation, characterization and in vitro evaluation of chicken feather fiber/thermoplastic polyurethane composites Özge Gökce, Murat Kasap, Gürler Akpmar, Güralp Özkoc, *J. Appl. Polym. Sci.* 2017, DOI: 10.1002/app.45338

Journal of Applied Polymer Science

Preparation, characterization, and *in vitro* evaluation of chicken feather fiber–thermoplastic polyurethane composites

Ozge Gokce,[1] Murat Kasap,[2] Gurler Akpinar,[2] Guralp Ozkoc [1,3]
[1]Department of Polymer Science and Technology, Kocaeli University, Kocaeli 41380, Turkey
[2]Department of Medical Biology, Kocaeli University, Kocaeli 41380, Turkey
[3]Department of Chemical Engineering, Kocaeli University, Kocaeli 41380, Turkey
Correspondence to: G. Özkoç (E-mail: guralp.ozkoc@kocaeli.edu.tr)

ABSTRACT: In this study, we aimed to investigate the potential use of keratin biofiber (KBF)-reinforced biodegradable thermoplastic polyurethane (TPU) composites as tissue engineering scaffolds. The composites were prepared by a solution casting method. Combined salt leaching and thermally induced phase-separation methods were used to manufacture porous scaffold structures. The mechanical properties were investigated with tensile tests and dynamic mechanical analysis (DMA). An increase in the fiber content increased the modulus and strength of the composites. The DMA results revealed that the storage modulus of the composites compared to that of the neat TPU was improved by the addition of feathers. Scanning electron microscopy analysis indicated that the dispersion of KBF in the TPU matrix was uniform. According to the water contact angle measurements, the hydrophilicity increased with increasing KBF content up to 80%. The thermal properties of the KBF–TPU films were measured by a differential scanning calorimetry method. The increase in the amount of KBF did not significantly affect the glass-transition temperature values. We examined the cytotoxicity and biocompatibility by performing cell culturing with the L929 mouse fibroblast cell line. The cell viability was found to be greater than 80% for all of the scaffold compositions. This showed that the KBF–TPU composite scaffolds may serve as a highly potent new material for skin tissue engineering applications. © 2017 Wiley Periodicals, Inc. J. Appl. Polym. Sci. **2017**, *134*, 45338.

KEYWORDS: biocompatibility; biomedical applications; composites; mechanical properties; polyurethanes

Received 8 January 2017; accepted 26 May 2017
DOI: 10.1002/app.45338

INTRODUCTION

Organ failure or loss as a result of any kind of damage or illness is a severe health issue, with the transplantation of an organ as a potential treatment option. Tissue engineering is a multidisciplinary field dealing with these problems through the combination of the principles of engineering and life sciences to generate a biological substitute that can improve, restore, and maintain tissue functions.[1,2] Because the highly promising field of tissue engineering is new, great effort is needed to transition laboratory-scale applications to industrial-scale applications. A common approach in tissue engineering is scaffold-guided tissue regeneration. In this approach, a scaffold acts as a porous three-dimensional matrix, which provides a culturing cell with an artificial extracellular matrix to guide cell growth and tissue regeneration by mimicking the extracellular matrix in real tissue. Some of the critical functions of a scaffold include the transportation of nutrients, removal of wastes, and diffusion of gases.[3,4]

Different natural polymers having the advantages of biocompatibility and nontoxicity, such as polysaccharides (e.g., cellulose and chitin) and proteins (e.g., collagen, elastin, fibrin, and keratin), have been used in the tissue engineering field. The disadvantages associated with natural polymers are their lack of reproducibility and unsatisfactory mechanical strength. Several synthetic polymers, such as polyglycolide, polylactide (PLA), poly(lactide-*co*-glycolide), and polyurethanes, have been used in the field of tissue engineering.[2] Polyurethanes are composed of aromatic or aliphatic isocyanate hard segments and polyester or polyether soft segments. The hardness, elastic modulus, and many other properties can be controlled by the ratio of soft segments to hard segments and the molecular weight of these segmental parts. Thanks to their biocompatibility, good barrier properties, and oxygen permeability, polyurethanes have been used extensively as biomaterials.[5]

Chicken feather, a byproduct from poultry, is composed of approximately 90% keratin, which is a protein-based natural biopolymer. Feather keratin, being a biodegradable, renewable, and potentially valuable biopolymer, consists of 50% fiber and 50% quill. Feathers can exist in two forms: α helixes and β sheets. The percentage of α-helix structures is higher than that

© 2017 Wiley Periodicals, Inc.

of β sheets. The quill part of the feather is aligned in β sheet, and the fibers have the α-helix structure.[6] It was suggested that feather keratin can be defined as a substrate for cell-culturing studies.[7] Although collagens are favorable in diverse forms for use in different fields,[8] there are higher risks for human response and the transfer of pathogens to the subject in clinical studies because the collagen originates from animal sources.[9] Keratin is a kind of intermediate filament specified as an intracellular cytoskeleton protein.[10] In addition, keratin is composed of the cell adhesion motif leucine–aspartate–valine amino acids (LDV), which behaves as an extracellular matrix substrate for cell attachment. For this reason, keratin can promote cell growth and cell spreading.[11] It was reported that mouse fibroblast cells were able to proliferate on keratin films, and this suggests their biocompatibility. In other words, keratin biofibers (KBFs) could be a good substrate for mammalian cell culturing.[12–14]

Some researchers have investigated the feather–polymer composites. Martinez-Hernandez *et al.*[15] investigated KBF-reinforced poly(methyl methacrylate) (PMMA) composites. The thermal properties and DMA results of the composites were evaluated. They reported that the transition temperatures and thermal stability were higher than that of standard PMMA. The storage modulus at room temperature increased. Amieva *et al.*[16] prepared chicken feather quill–recycled PP composites via an extrusion process. They investigated the effects of quill reinforcement on the density and thermal, thermomechanical, and morphological properties of the composites. They reported that for the lowest quill content, the composites showed an improved storage modulus in comparison to the neat polymer. In addition, the density of the composite materials was low. The transition temperature almost remained unchanged compared to that of polypropylene. Cheng *et al.*[17] examined the properties of PLA–chicken feather fiber composites. They used a twin-screw extruder to prepare chicken-feather-fiber-reinforced poly(lactic acid) composites. The tensile modulus was found to be higher for the composites than for the neat poly(lactic acid). The uniform distribution of fibers in PLA was evaluated by scanning electron microscopy (SEM) analysis. The results of the thermogravimetric experiments show that the thermal stability of the composites was enhanced by the addition of the fibers to the pure PLA. Zhan and Wool[18] investigated the properties of epoxy–chicken feather fiber–glass fiber composites. They showed that chicken feather fiber or hybrids with glass-fiber composites decreased the total density up to 30–40% compared to that of the glass-fiber composites. The chicken feather fibers had a lower aspect ratio compared to the glass fibers; this caused a decrease in the storage modulus of the chicken feather fibers. However, replacing the feather fibers partially with glass fibers increased the modulus and strength of the composites. Alagarsamy *et al.*[19] investigated the mechanical properties of coconut coir–chicken feather reinforced hybrid composites for potential use in the automobile industry. The composites were prepared via a hand-layup method with a polyester resin. They reported that the fiber percentage affected the mechanical properties, such as tensile strength, flexural strength, and impact strength, of the composites. As reported in the literature, the chicken-feather-based composites were prepared for commodity or structural applications but not for medical purposes. To the best of our knowledge, chicken feather KBF–polyurethane composites or scaffolds for possible tissue engineering applications have not been investigated. The purpose of this study was to prepare and characterize composites of KBF obtained from chicken feathers and poly(ε-caprolactone diol)-based biodegradable thermoplastic polyurethane (TPU) for potential use in spongy tissue scaffolds for the first time. The physical, mechanical, and thermal properties were investigated as a function of the KBF content for both bulk composites and spongy composites. The morphology of the scaffolds was investigated by SEM. In addition, *in vitro* cell-culturing studies were performed on the composite scaffolds to observe the potential biocompatibility of KBF.

EXPERIMENTAL

KBF–TPU Polymer Film Preparation

The TPU (Estane 54351 Nat021) was kindly obtained from Lubrizol Co. The KBFs were obtained from a local poultry farm in the Izmit region of Turkiye. The feather keratin fiber (number-average molecular weight = 10,500 g/mol) had a cysteine content of 7% in the amino acid sequence of feather keratin.[20] The chicken feathers were immersed in 95% EtOH for 1 h to remove the fat layer. Then, they were washed with 75% EtOH for 1 h to sterilize them. After sterilization, the KBFs were dried at 60 °C for 24 h. First, the larger quills were separated and then ground. Then, the KBFs were chopped with a kitchen-type grinder to an average length of 50 μm. The solution casting technique was used to prepare the KBF–TPU composites. Tetrahydrofuran was used as the solvent. The KBF content was varied as 0, 10, 20, 40, and 80 wt %. To distribute the feathers, the polymer solution–KBF mixture was mechanically stirred at 1000 rpm. After that, the solution was cast in a Petri dish to obtain a film having a thickness of 0.9 ± 0.1 mm.

Scaffold Preparation

Scaffolds were prepared for cell-culturing studies. The solvent casting–particulate leaching and thermally induced phase-separation methods were applied together to increase the porosity and interconnectivity.

An amount of 5 g of TPU was dissolved in 53.5 g of 1,4-dioxane (Merck KGaA) at 80 °C. A volume of 1 mL of water was added as a nonsolvent to induce liquid–liquid phase separation upon cooling. An amount of 21.5 g of NaCl crystals was sieved to a size of 125–250 μm and then added to polymer solution. The micrograph showing the length of KBF is shown in Figure 1. The average length of the fibers was obtained as 48.7 μm, and the diameter was 14.3 μm. To homogenize the mixture, we used a mechanical stirrer. The mixture was then transferred into a mold 25 mm in diameter and 10 mm in height. Then, it was frozen at −18 °C. Dioxane and water were evaporated in a freeze dryer at −110 °C *in vacuo* for 12 h. Salt was washed out from the polymer–salt mixtures for 24 h with 1 L of water/g of polymer. The scaffolds were finally dried in a vacuum stove at 37 °C for 24 h.[21]

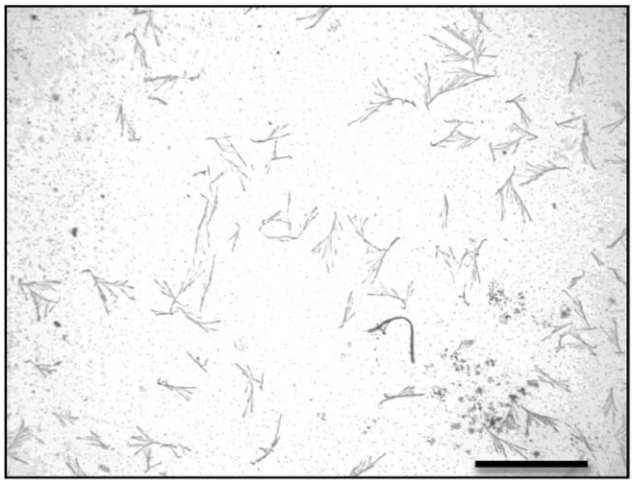

Figure 1. Picture of KBF fibers from optical microscopy (scale bar = 100 μm).

Tests for the KBF–TPU Composites

The dynamic mechanical properties were measured with a DMA50 01Db-Metravib instrument in tension mode. The frequency versus storage modulus was evaluated in the frequency range 0.1–200 Hz at a constant temperature of 37 °C. The strain was 0.3%, and the static force was 0.2 N.

Tensile testing was performed with a Tinius Olsen H5KT universal testing machine with standard dog-bone samples cut from the KBF–TPU films. The tests were conducted in saline buffer at 37 °C to mimic physiological conditions. The tensile strength was determined from the maximum stress measured during the tests. To obtain reproducible results, at least five parallel samples were tested.

Differential scanning calorimetry (DSC) was performed with a Mettler-Toledo DSC1 instrument to evaluate the thermal properties. Each KBF–TPU composite film was tested at a rate of 10 °C/min between −70 and 250 °C. Nitrogen gas was used as the purge gas.

The morphologies of the KBF–TPU films were investigated by SEM analysis with a JEOL JSM-6510 instrument. The samples were cryogenically fractured before analysis. The surfaces of the samples were sputter-coated with Au to prevent arching.

The surface wettabilities of the KBF–TPU composite films were assessed by water contact angle measurement with a KSV Attention Tetalite instrument.

Tests for the Porous KBF–TPU Scaffolds

The KBF–TPU scaffolds were characterized to observe the pore characteristics, mechanical properties, and *in vitro* biocompatibility with mouse fibroblast cells (L929). A Trypan Blue exclusion assay was used to determine the number of viable cells in a cell suspension. SEM analysis was performed to observe cell attachment on the scaffolds.

The L929 fibroblast cells were routinely cultured in Dulbecco's modified Eagle's medium (DMEM) containing high glucose supplemented with fetal bovine serum (FBS) at 10% and 50 mg/mL streptomycin in 50 mL plastic culture flasks. They were subcultured every 4 days. A 0.2% trypsin/0.02% ethylene diamine tetraacetic acid mixture was used to treat the cells in the logarithmic growth phase. Then, the cells were washed with DMEM containing 10% FBS, collected by centrifugation at 1000 rpm for 3 min, and resuspended in DMEM containing 10% FBS at 2.5×10^5 cells/mL. A concentration of 5×10^4 cells per cell culture plate was seeded onto each dish and cultivated at 37 °C in an incubator under humidified 5% CO_2. The adhesion and proliferation of cells were monitored under a phase-contrast microscope (Olympus, CK2, Japan). After incubation for a defined period, the cells on the scaffolds were detached by a 0.2% trypsin treatment and counted with a hemocytometer for cell viability measurement in the Trypan Blue exclusion assay according to ISO 10993-5. The principle of the Trypan Blue exclusion assay is based on the fact that live cells possess intact cell membranes that exclude certain dyes, such as Trypan Blue; on the other hand, dead cells do not. A cell suspension obtained from the medium that was previously in contact with the scaffold was mixed with the dye. Then, the cells were visually observed to determine whether they were taking or excluding the dye.

SEM (JEOL JSM-6510) was used to investigate the scaffold pore characteristics and L929 cell morphology. For the cell morphological analysis, KBF–TPU scaffolds after 12 h of cell seeding were fixed with 2.5% glutaraldehyde (Sigma-Aldrich Co.) for 4 h. Then, they were dehydrated in a graded EtOH series of 25, 50, 75, and 95% for 5 min for the first one and 10 min for the rest. The samples were further dehydrated in pure EtOH three times, then air-dried, and gold-sputtered under a high vacuum.

The scaffold porosity was calculated from the following equations:

$$M_0 = V_0 \times \rho_0 \quad (1)$$

$$M_{pores} = M_0 - M_{scaffold} \quad (2)$$

$$V_{pores} = M_{pores}/\rho_0 \quad (3)$$

where $M_{scaffold}$, the mass of scaffold, was measured by an analytical precision balance, M_0 is the bulk mass of the scaffold before leaching with a volume V_0 and a density ρ_0, M_{pores} is the weight of the pores after leaching, and V_{pores} is the volume of the pores.

The porosity then was calculated by eq. (4):

$$\text{Porosity } (\%) = [V_{pores}/V_0] \times 100 \quad (4)$$

Compression tests were done with cylindrical specimens 15 mm in diameter. They were punched manually from the KBF–TPU scaffolds. The temperature of the environment was 21 °C, and the strain rate was 2 mm/min. The tests were done with a Lloyd texture analyzer. The compression modulus was determined at 2% compression.

RESULTS AND DISCUSSION

Table I shows the changes in the complex modulus and tensile strength with respect to the KBF content. Because the modulus and strength of feathers were higher than those of TPU,[15] the composites exhibited improved modulus and strength in comparison to the neat TPU. We found that the increase in the fiber content enhanced the modulus in the entire range and the strength of the composites up to 40% KBF. As the fiber content

Table I. Mechanical Properties of the KBF–TPU Composites

	KBF content (w/w %)				
Property	0	10	20	40	80
Complex modulus at 1 Hz (MPa)	75	110.1	199.9	194.6	60.4
Tensile strength (MPa)	5.1	18.9	20.5	28.7	22.8
Elongation at break (%)	210	224	276	273	183

increased to 20 and 40%, up to a 2.6-fold increase in the modulus was obtained. A similar phenomenon was also observed for the tensile strength. The increase in the tensile strength at 10% was about 0.45-fold over that of the neat matrix. General composite theories explained the properties of a brittle fiber embedded in a ductile matrix system. If the fiber content is lower than the minimum required volume faction, the stress on a composite can break the fibers, which can be treated as voids that reduce the strength of the composites or do not have a positive effect.[22,23] At 80% KBF content, because of the higher volume fraction of fibers, or in other words, because of the insufficient TPU, the matrix continuity was lost, and a no longer uniform TPU distribution was achieved. Therefore, the strength and elongation at break were lowered at 80%. This was associated with the fact that as the fiber content increased, because of the lower amount of the polymer matrix, the stress could be transferred from the matrix to the fibers at small strains, but for the high strains, because of the lack of sufficient interactions between the matrix and fiber, the stress-transfer efficiency was very low. Therefore, the modulus improved because it was measured at very small strains, but the strength and elongation decreased. One of the other concerns here was the localized nonuniform orientation of the fiber distribution, which had a negative effect on the mechanical properties. Because of the elastomeric nature of TPU, the elongation at break values of the composites were still high, despite the addition of rigid KBF. The fibers bridged the crack tips, and this retarded the fracture process of the composite. In other words, the failure of the composite depended on the bridging effect of KBF inside the composite, and the risk of sudden failure was reduced.

To obtain a homogeneous and sufficient cell seeding, the wettability of the polymer scaffold plays a crucial role. Because the biodegradable synthetic polymers are mostly not hydrophilic, the delivery of a cell suspension uniformly through a porous scaffold is difficult.[24] It is known from the amino acid sequence of feather keratin that the protein has 40% hydrophilic groups.[25] To judge the surface hydrophilicity of the composites, the water contact angles of the KBF–TPU composites were measured (Table II). We observed that the hydrophilicity increased with increasing KBF content up to 80%. The increasing hydrophilicity could have arisen from the hydrophilicity of the keratin, which absorbed water as unbound water. Because of the nonhomogeneous surface roughness of the composite having 80% KBF, the contact angle could not be measured.

Table II. Water Contact Angles of the KBF–TPU Composites

KBF content (%)	Water contact angle (°)
0	94.5 ± 2.3
10	73.8 ± 1.7
20	69.5 ± 2.8
40	59.4 ± 3.0

The SEM micrographs of the fracture surfaces of the KBF–TPU composites are shown in Figure 2. We observed that fibers were coated with a layer of polymer, and the fracture occurred in the polymer phase; this indicated a good compatibility and good adhesion at the interphase (as shown by yellow arrows). When the fibers were pulled out, some matrix deformation also simultaneously occurred. From the voids and the exposed fibers, we noticed that some of the fibers were pulled out. In addition, as an indication of strong fiber–polymer interactions, we observed that some of the fibers were broken in the same fracture plane as the polymer. As shown in Figure 2, the fracture morphology was ductile with some localized plastic deformation of the polymer.

The thermal properties of the KBF–TPU composite films were determined by DSC. The glass-transition temperature (T_g), melting temperature (T_m) values, and melting enthalpy were determined from the DSC heating curves (Table III). As shown, the increase in the amount of KBF did not cause a significant change in the T_g values (ca. −40 °C) of the TPU. T_g of neat KBF was found to be 232.8 °C; this was consistent with the literature.[15] The reason for this high T_g of KBF was the hydrogen-bonded α-helix structure of keratin, which yielded very high chain packing. The crystalline T_m of the hard segments of TPU was observed at 176.6 °C. The addition of KBF to the matrix deteriorated the crystallization of TPU; therefore, all of the KBF–TPU composites were in the amorphous phase.

Several researchers have investigated the state of water absorbed in biological polymers with various techniques. Specific interactions and the chain structure affects the water in polymeric materials, for example, the water that does not freeze as a result of strong hydrogen bonding with polymers. This kind of water is called *bound water*. Bound water evaporates at elevated temperatures because of strong hydrogen bonds. Keratin fibers may contain both freezing water and bound water that is hydrogen-bonded to the peptide bonds. The broad water loss endotherms around 60–110 °C were a good indication of this phenomena (Figure 3). It was also revealed from the DSC curves that the addition of keratin fibers increased the water content of the composites. This may be an advantage for potential wound-healing materials applications because the moisture of the

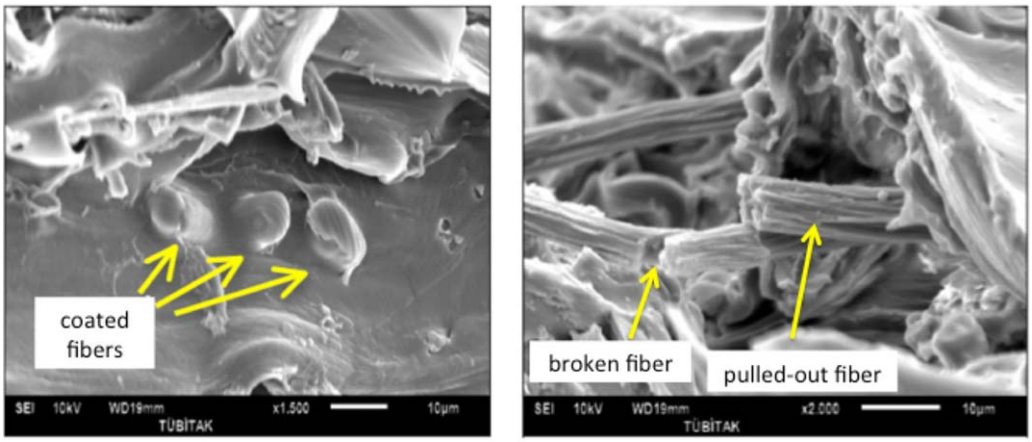

Figure 2. SEM micrographs of the KBF–TPU composites: (A) 10% KBF and (B) 40% KBF. [Color figure can be viewed at wileyonlinelibrary.com]

Table III. Thermal Properties of the KBF–TPU Composites

	T_g (°C)	$T_{water\ loss}$: Onset and end-set temperatures (°C)	$\Delta H_{water\ loss}$ (J/g)	T_m (°C)
Neat TPU	−40.9	—	—	176.6
10%KBF-90%TPU	−41.1	14.7-116.9	23.1	—
20%KBF-80%TPU	−42.1	12.2-105.9	34.1	—
40%KBF-60%TPU	−41.8	11.5-126.7	41.2	—
80%KBF-20%TPU	−44.5	41.7-135.9	78.8	—
Neat KBF	232.8	98.5-101.1	99.9	—

wound is very important in the healing process. At temperatures above 230 °C, keratin denaturation was observed in all of the DSC thermograms and was seen as multiple endotherms. For example, the denaturation of the 40%KBF–60%TPU composite started around 230 °C, and that of 80%KBF–20%TPU composite started around 240 °C. An example is shown in Figure 3. Similar observations were reported for chicken-feather-doped PMMA in several studies.[26,27]

The cell-culturing studies were performed on porous keratin–TPU scaffolds prepared via particle leaching in combination with a thermally induced phase-separation technique. The resulting spongy structures were highly porous with an even pore distribution. The interconnected pore structures are shown in Figure 4. The interconnectivity and porosity seemd to increase with increasing fiber content. The larger pores resulted from the particle leaching of the salt, and small pores were obtained from the evaporation of dioxane and tetrahydrofuran during freeze drying. An interconnected pore structure and high porosity were successfully achieved with combination of these two methods as also represented by Heijkants *et al.*[21]

The porosity of the scaffolds was obtained according to the method described in the Experimental section and summarized in Table IV. The results show that the average porosity of the scaffolds was higher than 80% without any significant difference with respect to composition. As mentioned in the literature, a porosity value of more than 65% allows the scaffold mass transfer and transport of gases.[28] In addition, it is also an important feature to have an interconnected pore network. Therefore, the results of porosity were enough for nutrient and waste transfer, and also, the scaffolds could be considered for tissue engineering skin-dressing materials.[28] The results were consistent with the cell-culturing assays mentioned in the next part.

Moreover, the pore size is another important feature. It has been stated that the pore size should be in the 50–500 μm range for vascularization and regeneration of the tissue. The SEM photographs showed that the pore sizes of the KBF–TPU scaffolds were about 50–350 μm, as shown in Figure 4.[28] In addition, they were well connected to each other.

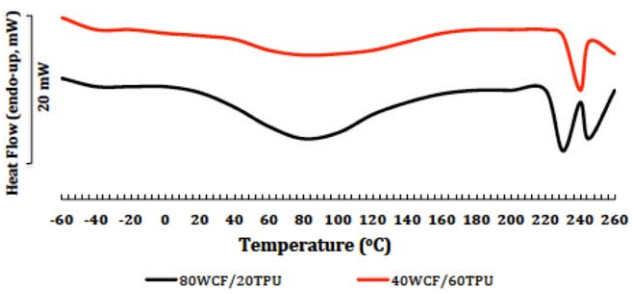

Figure 3. Representative DSC curves of KBF. [Color figure can be viewed at wileyonlinelibrary.com]

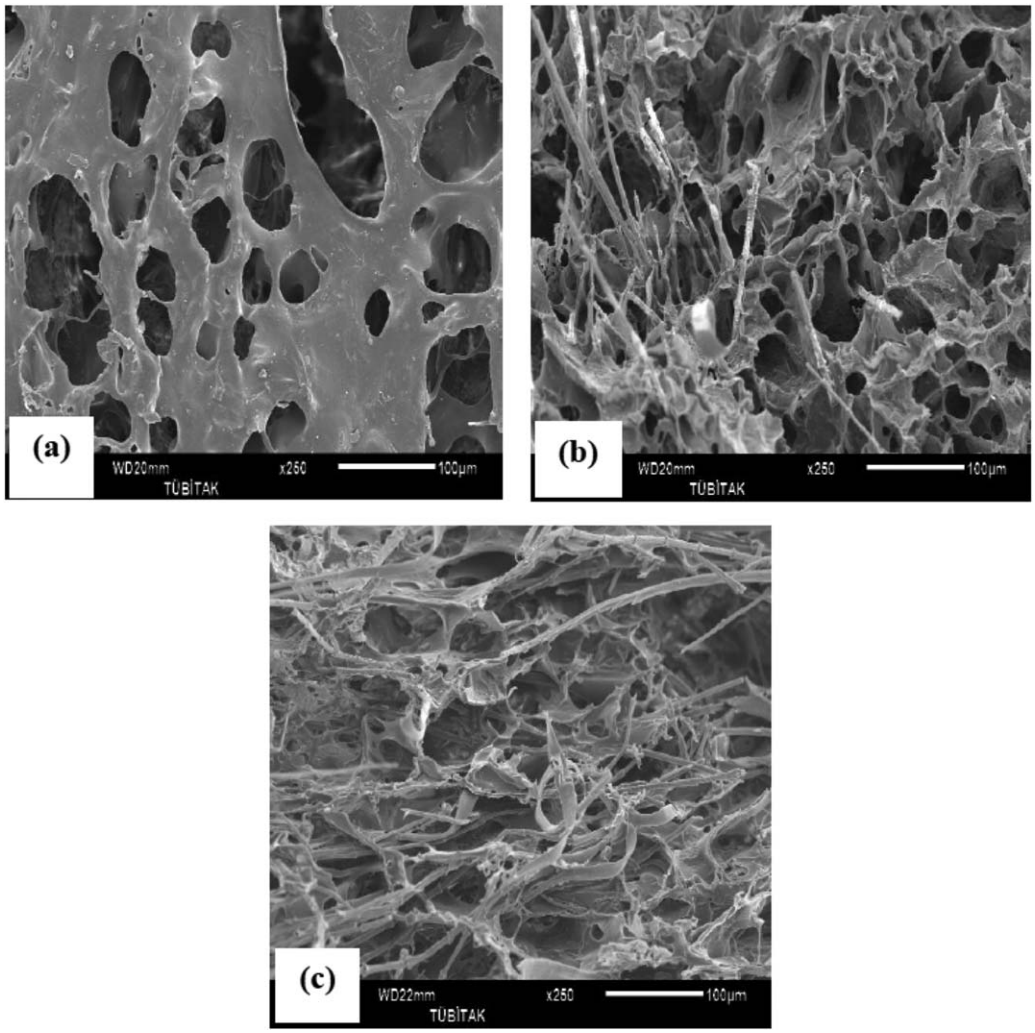

Figure 4. SEM micrographs of the KBF–TPU scaffolds (250×, scale bar = 100 µm): (a) neat TPU, (b) 20KBF–80TPU, and (c) 80KBF–20TPU.

The elastic modulus of the KBF–TPU scaffolds in the compression test was measured at 2% strain. Because of complex interactions between local failures and structural instabilities, the compression test of a fiber-reinforced porous composite specimen can be considered as a structural test.[29] In the compression test, several failure mechanisms, for example, fiber crushing, matrix failure, fiber pullout, and fiber kinking, can occur independently or interact with each other. In this study, the elastic modulus improved with increasing KBF content above 20%, as shown in Figure 5. Because the level of porosity was similar, the most dominant parameter was the fiber content. The reasons for this improvement were associated with the percolation of KBF above a certain loading level[21] and the intrinsically higher modulus of feathers in comparison to the matrix.

To examine the biocompatibility of the composite scaffolds, L929 fibroblasts cultured in Dulbecco's modified Eagle's medium (DMEM) containing high glucose were seeded onto

Table IV. Porosity of the Scaffolds

Scaffold composition	Porosity (%)
10KBF-90TPU	86.5 ± 4.2
20KBF-80TPU	93.2 ± 2.3
40KBF-60TPU	87.7 ± 3.6
80KBF-20TPU	80.4 ± 2.1

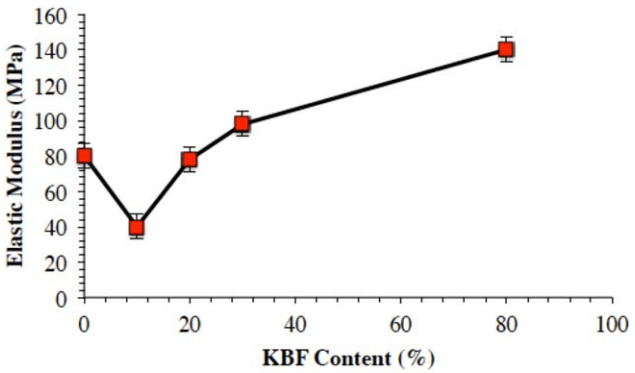

Figure 5. Elastic modulus obtained from the compression testing of the KBF–TPU scaffolds. [Color figure can be viewed at wileyonlinelibrary.com]

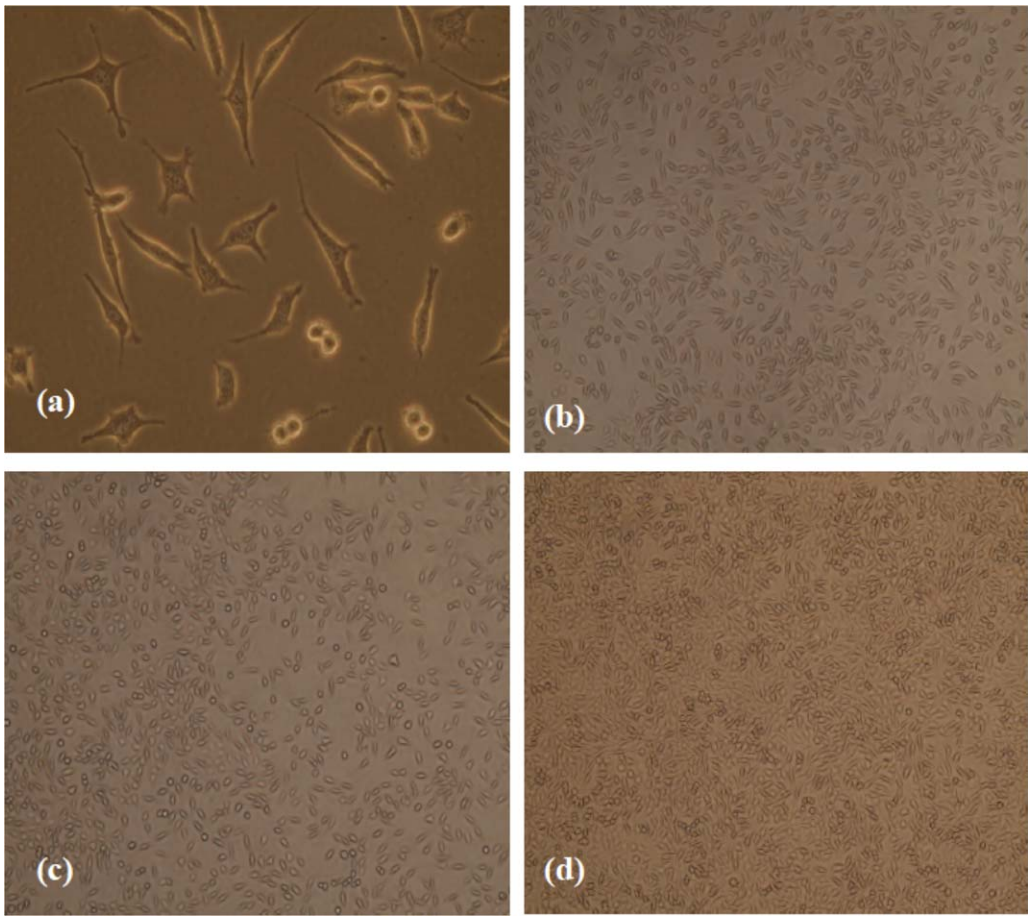

Figure 6. (a) L929 cell line morphology (40×) and (b–d) cell spreading on day 3 (110×), day 5 (4×), and day 7 (10×), respectively. [Color figure can be viewed at wileyonlinelibrary.com]

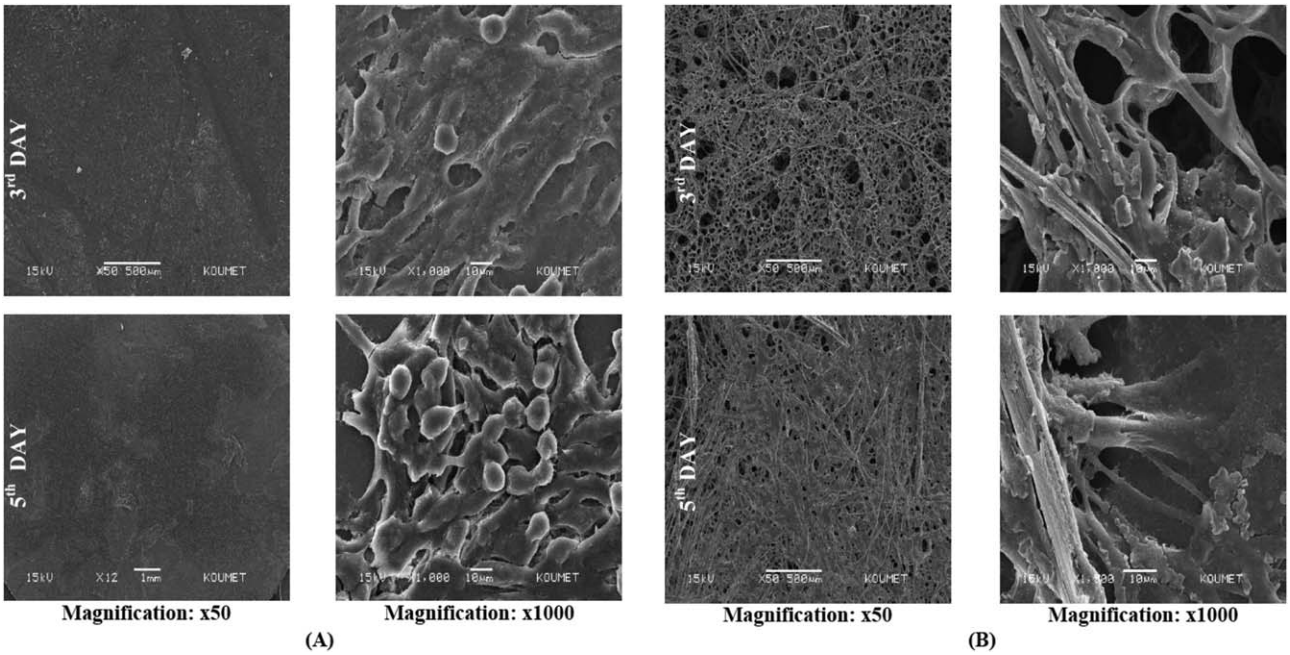

Figure 7. SEM micrographs of the cell-seeded (A) neat TPU and (B) 20KBF–80TPU scaffolds.

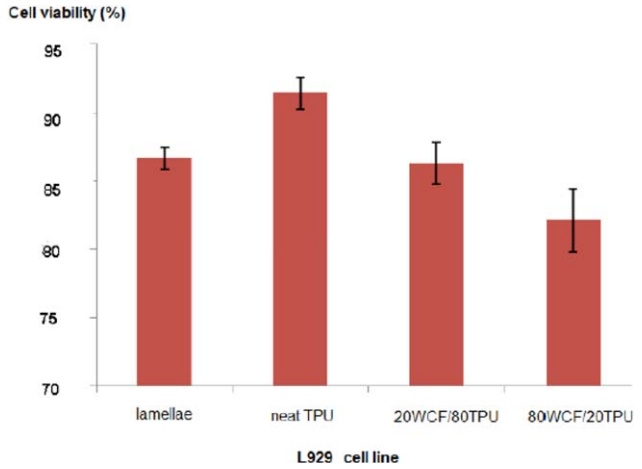

Figure 8. L929 cell viability on the scaffolds. [Color figure can be viewed at wileyonlinelibrary.com]

neat TPU films; 20KBF–80TPU, 40KBF–60TPU, and 80KBF–20TPU scaffolds; and lamellae as a positive control. The L929 fibroblast cell morphology was observed under light microscopy, as shown in Figure 6. After the 3rd and 5th days of culturing, SEM micrographs of the fibroblast-seeded materials were taken (Figure 7). We observed that the L929 fibroblast cells were able to grow and proliferate with an almost extended shape on the scaffold surfaces. The morphologies of those fibroblasts were spherical on a smooth surface of neat TPU [Figure 7(A)] and flattened on rough surface of the scaffolds, as shown in Figure 7(B). We also observed that some extracellular matrixes appeared around the cells and cell groups. These findings were consistent with those in the literature.[30]

The number of viable cells present in the cell suspension was determined with the Trypan Blue exclusion test. Figure 8 shows the L929 cell line viability on the composite scaffolds. On the surface of the lamellae and scaffolds, the cell viability was greater than 80% for all of the scaffolding materials. A greater than 80% cell viability is considered possibly biocompatible and nontoxic. Therefore, it is thought that when subcutaneously embedded in mice, this composite scaffold would not cause any inflammatory or immunological responses and would be biodegradable indeed.[31]

CONCLUSIONS

KBF-fiber-reinforced TPU composites were prepared and characterized. The fiber content was found to be the most important parameter in terms of the mechanical properties of the composites. As the fiber content increased beyond 40%, the mechanical properties decreased because of the loss of continuity of the matrix. The wettability and water content of the composites were improved by the addition of KBF. The scaffold structure was highly porous, and the pores were evenly distributed and interconnected. Cell-culturing studies showed that the cells grew and proliferated with an almost extended shape, a little like a monolayer culture on the scaffold surface. The cell viability test indicated that for all of the KBF–TPU scaffolds, the cell viability was greater than 80%. This cell viability is enough the scaffolds to be used as biomaterials. As a general conclusion, it was demonstrated that KBF–TPU could be used as a potential biomaterial for tissue engineering scaffolds.

REFERENCES

1. Ratcliffe, A. *Matrix Biol.* **2000**, *19*, 353.
2. Skarja, G. A.; Woodhouse, K. A. *J. Polym. Sci.* **2000**, *75*, 1522.
3. Mikos, A. G.; Thorsen, J. A.; Czerwonka, L. A.; Langer, R. *Polymer* **1994**, *38*, 1068.
4. Heather, P. M. Ph.D. Thesis, Ohio State University, **2004**.
5. Lamba, N. M. K.; Woodhouse, K. A.; Cooper, S. L. Polyurethanes in Biomedical Applications; CRC Press: Boca Raton, FL, **1998**.
6. Ullah, A.; Wu, J. *Macromol. Mater. Eng.* **2013**, *298*, 153.
7. Wang, S.; Taraballi, F.; Tan, L. P.; Ng, K. W. *Cell Tissue Res.* **2013**, *347*, 795.
8. Meena, C.; Mengi, S. A.; Deshpande, S. G. *Chem. Sci.* **1999**, *111*, 319.
9. Song, E.; Kim, S. Y.; Chun, T.; Byun, H. J.; Lee, Y. M. *Biomaterials* **2006**, *27*, 2951.
10. Szeverenyi, I.; Cassidy, A. J.; Chung, C. W.; Lee, B. T.; Common, J. E.; Ogg, S. C.; Chen, H.; Sim, S. Y.; Goh, W. L.; Ng, K. W.; Simpson, J. A.; Chee, L. L.; Eng, G. H.; Li, B.; Lunny, D. P.; Chuon, D.; Venkatesh, A.; Khoo, K. H.; McLean, W. H.; Lim, Y. P.; Lane, E. B. *Hum. Mutat.* **2008**, *29*, 351.
11. Verma, V.; Verma, P.; Ray, P.; Ray, A. R. *Biomed. Mater.* **2008**, *3*, 12.
12. Yamauchi, K.; Maniwa, M.; Mori, T. *J. Biomater. Sci. Polym. Ed.* **1998**, *3*, 259.
13. Tanebe, T.; Okitsu, N.; Tachibana, A.; Yamauchi, K. *Biomaterials* **2002**, *23*, 817.
14. Katoh, K.; Shibayama, M.; Tanabe, T.; Yamauchi, K. *Biomaterials* **2004**, *25*, 2265.
15. Martinez-Hernandez, A. L.; Velasco-Santos, C.; Victos de, I. M.; Castano, M. *Compos. B* **2007**, *38*, 405.
16. Amieva, E. J.-C.; Velasco-Santos, C.; Martinez-Hernandez, A. L.; Rivera-Armenta, J. L.; Mendoza-Martinez, A. M.; Castano, V. M. *J. Compos. Mater.* **2015**, *49*, 275.
17. Cheng, S.; Lau, K.; Liu, T.; Zhao, Y.; Lam, P. M.; Yin, Y. *Compos. B* **2009**, *40*, 650.
18. Zhan, M.; Wool, R. P. *J. Appl. Polym. Sci.* **2016**, *133*, DOI: 10.1002/app.44013.
19. Alagarsamy, S. V.; Arockia, V. S. S.; Vignesh, S. *Int. J. Sci. Eng. Technol. Res.* **2015**, *4*, 12.
20. Barone, J. R.; Schmidt, W. F. *Compos. Sci. Technol.* **2005**, *65*, 173.
21. Heijkants, R. G. J. C.; Van Tienen, T. G.; De Groot, J. H.; Pennings, A. J.; Buma, P.; Veth, R. P. H.; Schouten, A. J. *J. Mater. Sci.* **2006**, *41*, 2423.
22. Shah, D. U.; Schubel, P. J.; Licence, P.; Clifford, M. *J. Compos. Sci. Technol.* **2012**, *72*, 1909.

23. Harris, B. Engineering Composite Materials; Institute of Materials: London, UK, **1999**.
24. Chen, G.; Ushida, T.; Tateishi, T. *Mater. Sci. Compos.* **2001**, *17*, 63.
25. Murayama-Arai, K.; Takahashi, R.; Yokote, Y.; Akahane, K. *Eur. J. Biochem.* **1983**, *132*, 501.
26. Fried, J. R. Polymer Science and Technology, 2nd ed.; Prentice Hall: Upper Saddle River, NJ, **2003**; p 582.
27. Tang, Z. G.; Black, R. A.; Curran, J. M.; Hunt, J. A.; Rhodes, N. P.; Williams, D. F. *Biomaterials* **2004**, *25*, 4741.
28. Katoha, K.; Tanabe, T.; Yamauchi, K.; *Biomaterials* **2004**, *25*, 4255.
29. Herakovich, C. T. Mechanics of Fibrous Composites; Wiley: New York, **1998**.
30. Ma, J.; Wang, H.; He, B.; Chen, J. *Biomaterials* **2001**, *22*, 331.
31. Yamauchi, K.; Yamauchi, A.; Kusunoki, T.; Kohda, A.; Konishi, Y. *J. Biomed. Mater. Res.* **1996**, *4*, 439.